DOI: 10.2478/rjti-2018-0013
ROMANIAN JOURNAL
OF TRANSPORT INFRASTRUCTURE

SIMULTANEOUS INFLUENCE OF THE TRACK AXIS CURVATURE AND THE SUPPORT LINE OBLIQUITY AT RAILWAY BRIDGE SUPERSTRUCTURES WITH STEEL BEAMS EMBEDDED IN CONCRETE

Stănescu Răzvan Marian, Assistant Lecturer, PhD, Faculty of Railways, Roads and Bridges, Technical University of Civil Engineering Bucharest, Romania;
Stan Oana Mihaela, Lecturer, PhD, Faculty of Railways, Roads and Bridges, Technical University of Civil Engineering Bucharest, Romania.

Rezumat

Pentru domeniul deschiderilor mici (L≤35.00m) la podurile feroviare noi se recomandă şi se utilizează suprastructurile cu grinzi metalice înglobate în beton, cu care se pot asigura exigenţele de rezistenţă şi mai ales de rigiditate, indiferent de viteza de circulaţie.

În toate prescripţiile de proiectare existente până în prezent pentru structurile de poduri cu grinzi metalice înglobate în beton, şi, chiar în literatura tehnică de specialitate, există puţine informaţii şi date referitoare la influenţa oblicităţii rezemării şi a curburii axei căii în concepţia şi calculul acestor tipuri de structuri.

În prescripţiile de proiectare calculul este unul simplificat, realizat pe o singură grindă longitudinală izolată din tablier, dacă se îndeplinesc anumite condiții legate de geometria structurii (oblicitate, curbură). Dacă aceste condiții nu sunt îndeplinite se recomandă analiza cu programe de element finit.

Articolul își propune să studieze situațiile în care nu sunt îndeplinite condițiile prescripţiilor de proiectare.

Cuvinte cheie: oțel, beton, curbură, oblicitate.

Abstract

For new railway bridges with small spans (L ≤ 35.00 m) superstructures with steel beams embedded in concrete are recommended and used, which can ensure the requirements of strength and especially stiffness, regardless of velocity.

In all the design prescriptions used so far for superstructures with steel beams embedded in concrete, and even in the technical literature, there is little information and data on the influence of the support line obliquity and the track axis curvature in the design and calculation of these types of structures.

In the design code, if certain conditions related to the geometry of the superstructure are met (obliquity, curvature) the calculation is a simplified one, made on a single isolated longitudinal beam of the deck; otherwise, if the conditions are not met, finite element program analysis is recommended.

The article aims to study the situations in which the requirements of the design prescriptions are not met.

Keywords: steel, concrete, curvature, obliquity.

1. PRESENTATION OF BRIDGE STRUCTURES ANALYZED [4]

Three simple supported bridges with steel beams embedded in concrete, with L=10m, L=20m and L=30m spans, were chosen for the study. For these, the support line obliquity (40^G, 50^G and 60^G) and the track axis curvature (100m ... 1500m) were varied.

The *Design Tables for Filler Beam Railway Bridges* [4], published by the International Union of Railways, has been the guideline for the constructive solutions of the three analyzed bridges. For the bridge with L=10m span and a B track category, at a maximum speed of 160Km/h, the constructive solution consists of six steel beams HEA400 in cross-section, as shown in Figure 1. For the bridge with L=20m span the constructive solution consists of six HEB800 steel beams (see Figure 2) and for the bridge with L=30m span the constructive solution consists of six HLB1100 steel beams (see Figure 3).

In all three cases a deck width of 4m was obtained.

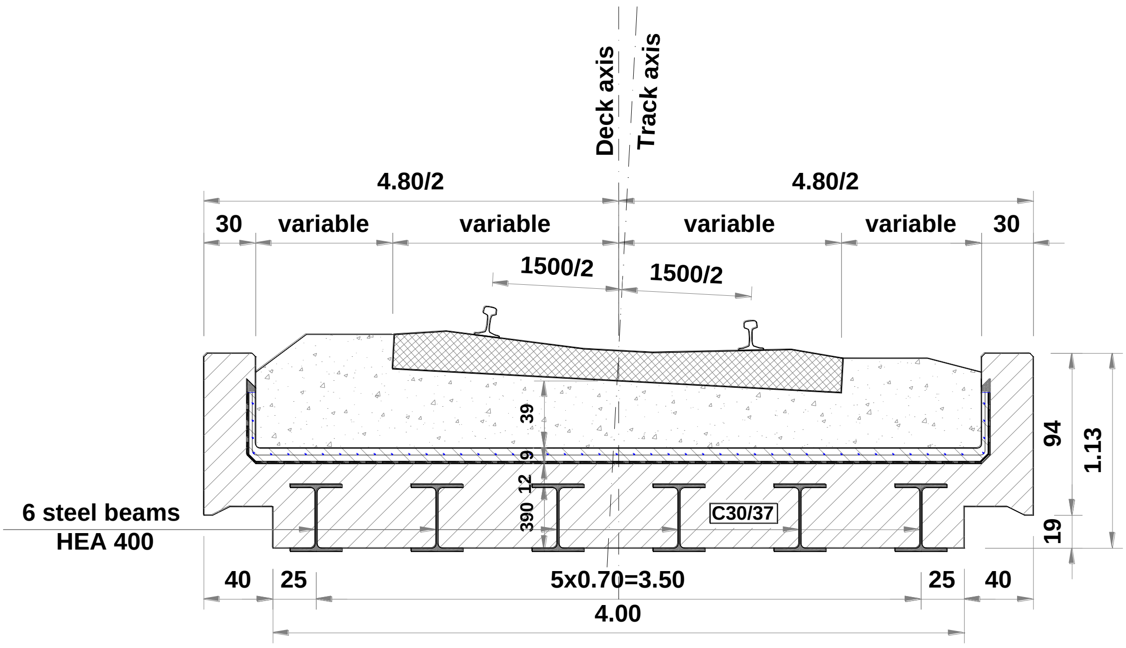

Figure 1. Constructive solutions for bridge with L=10m span

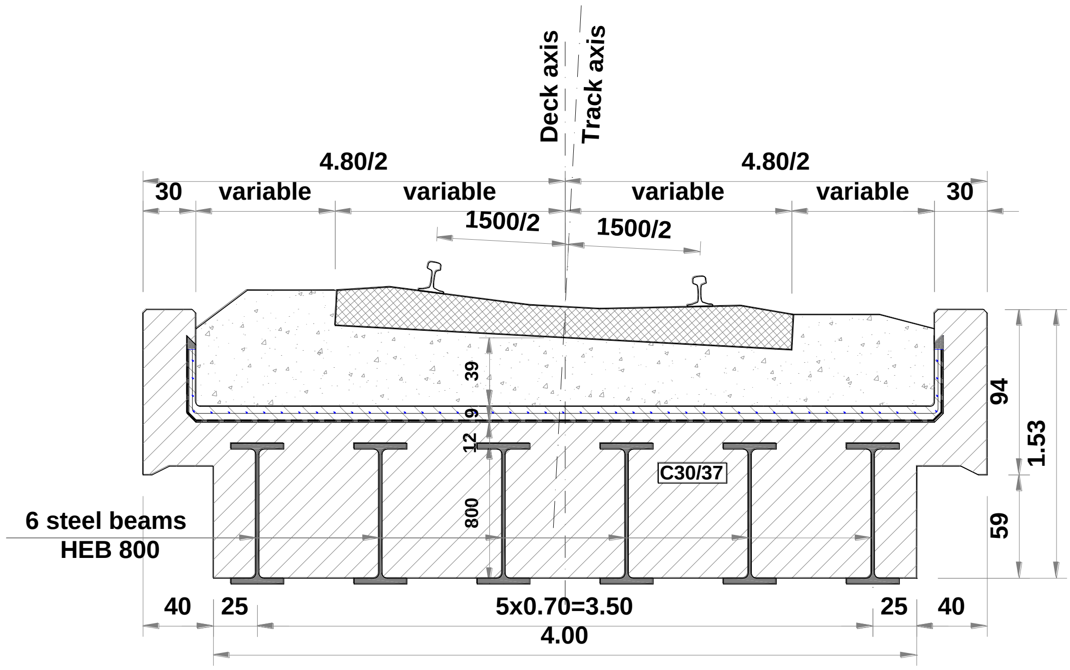

Figure 2. Constructive solutions for bridge with L=20m span

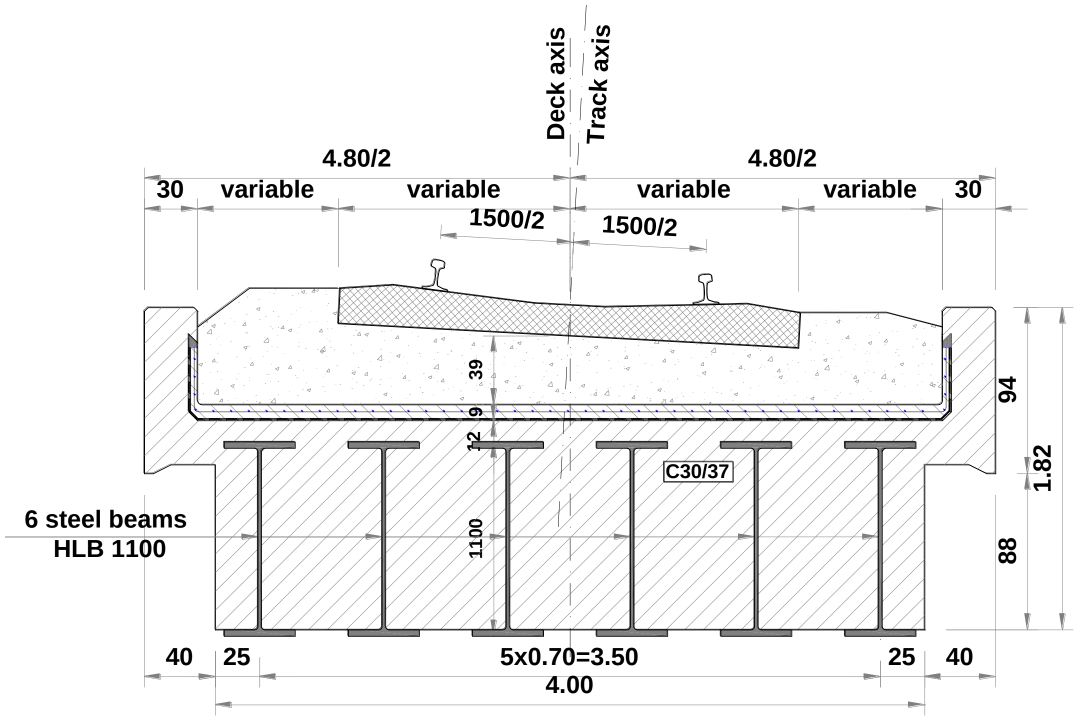

Figure 3. Constructive solutions for bridge with L=30m span

2. PRESENTATION OF THE CALCULATION MODELS [4]

Structures were analyzed with the Lusas FEA software, using 3D type "Stress" finite elements to model them.

To be able to observe the influence of support line obliquity and track axis curvature, bridges were first analyzed without support line obliquity and in alignment.

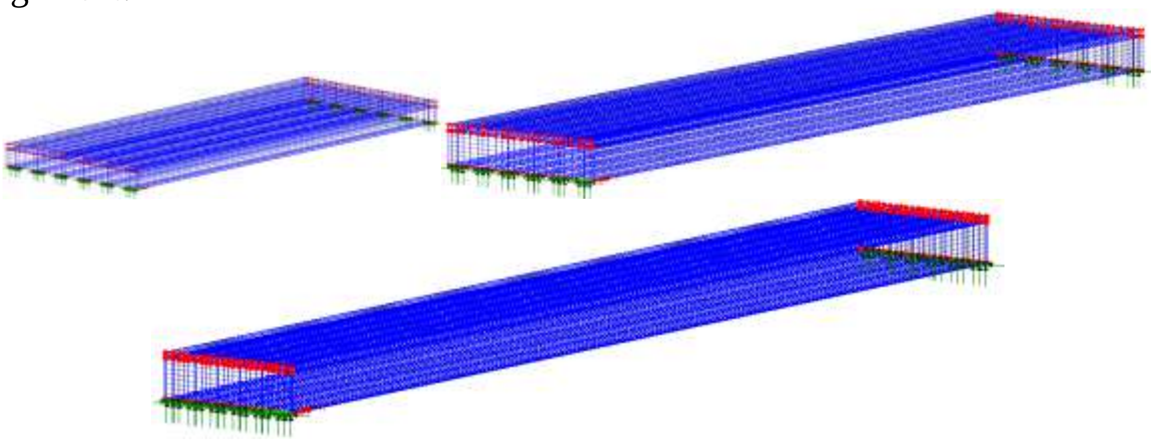

Figure 4. 3D view of the calculation models for bridges with 10m, 20m and 30m spans without support line obliquity

- **Bridge with L=10m span**

The calculation model contains 23200 "3D" finite elements type "Stress" HX8M and 28674 nodes, resulting 86022 degrees of freedom, as shown in Figure 5.

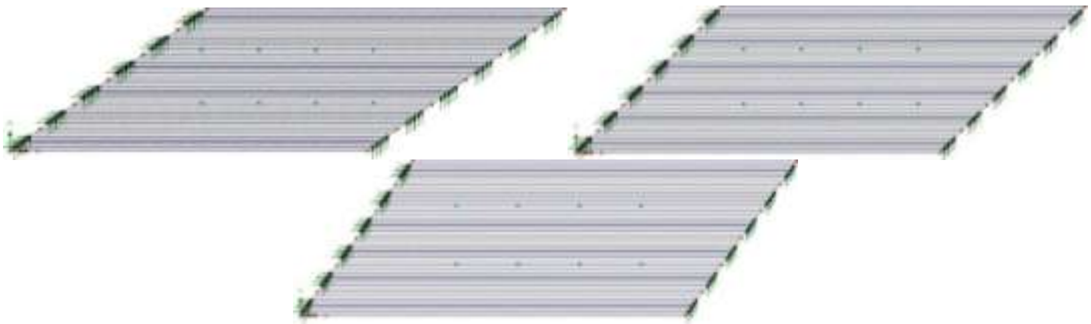

Figure 5. Plane view of the calculation models for bridge with 10m span and 40^G, 50^G and 60^G support line obliquity

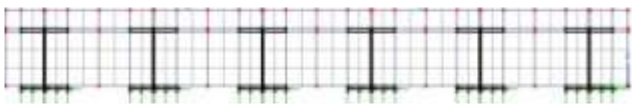

Figure 6. The cross-section of the bridge with L=10m span

- **Bridge with L=20m span**

The calculation model contains 47880 “3D” finite elements type "Stress" HX8M and 57387 nodes, resulting 172161 degrees of freedom (see Figure 7).

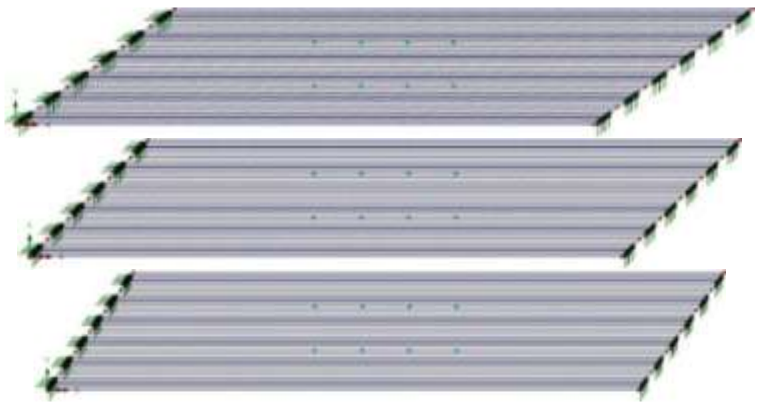

Figure 7. Plane view of the calculation models for bridge with 20m span and 40^G, 50^G and 60^G support line obliquity

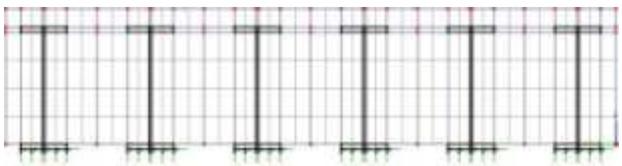

Figure 8. The cross-section of the bridge with L=20m span

- **Bridge with L=30m span**

The calculation model contains 51600 “3D” finite elements type "Stress" HX8M and 60903 nodes, resulting 182709 degrees of freedom (see Figure 9).

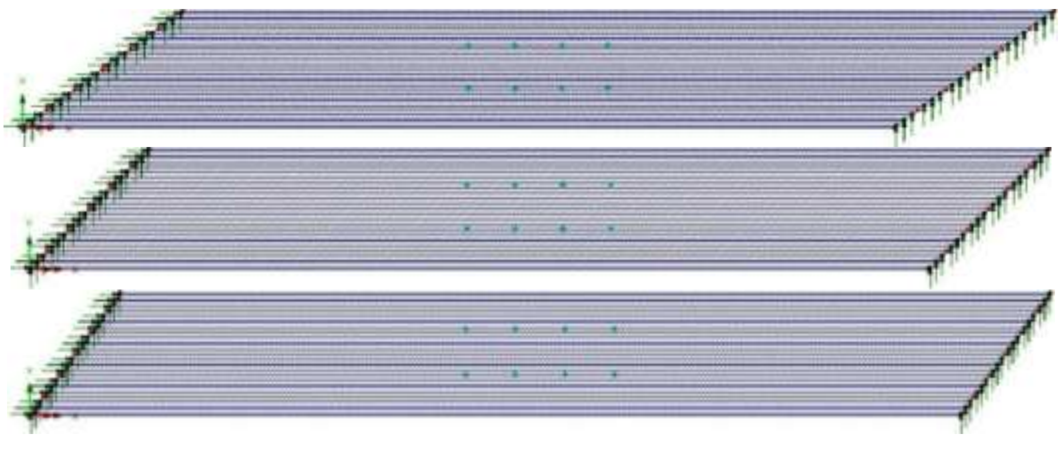

Figure 9. Plane view of the calculation models for bridge with 30m span and 40^G, 50^G and 60^G support line obliquity

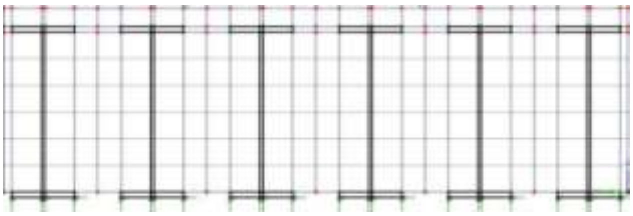

Figure 10. The cross-section of the bridge with L=30m span

The calculation models were analyzed under the effect of permanent loads and the LM71 convoy.

3. SUMMARY PRESENTATION OF THE RESULTS OBTAINED USING THE LUSAS FEA SOFTWARE

From the analysis the following sizes proposed to be compared were extracted:

- Maximum deflection of the deck from permanent loads and LM71;
- Bending moments from permanent loads and LM71 in the midspan on each isolated longitudinal composed beam from the deck.

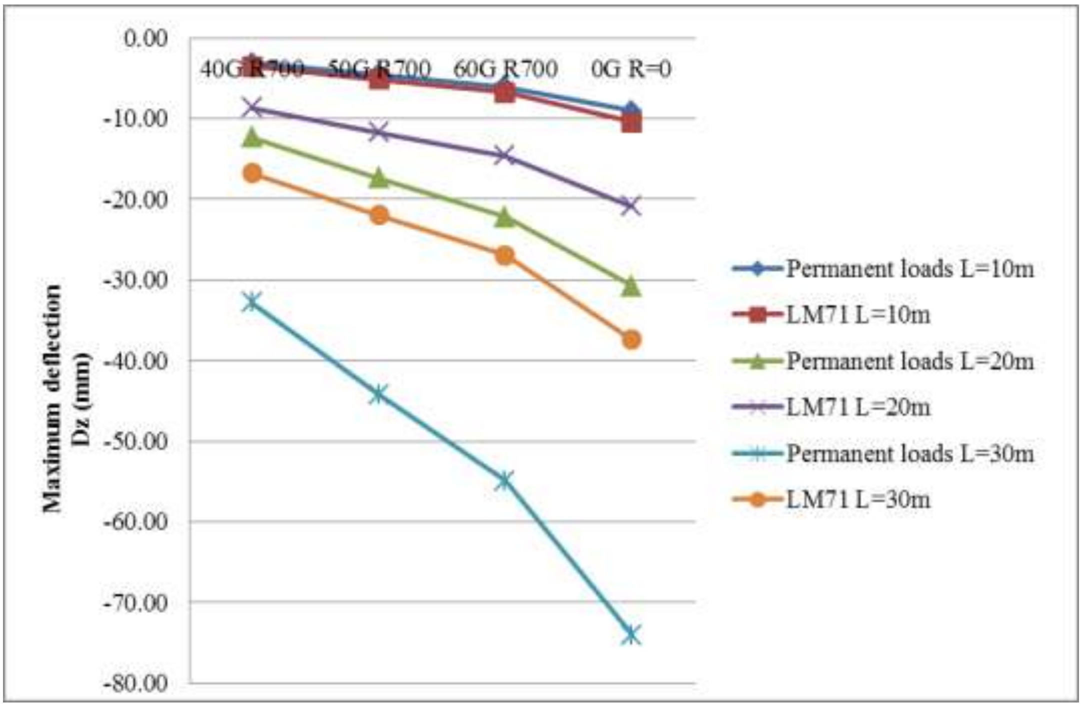

Figure 11. Maximum deflection variation depending on deck support line obliquity and bridge span for R=700m

Table 1. Maximum deflection of the deck (ΔZmax)

L	Obliquity	Radius	ΔZmax Permanent loads	ΔZmax LM71
L=10m opening	40^G	R=100m	-3.01	-3.30
		R=700m	-3.05	-3.54
		R=1500m	-3.04	-3.38
	50^G	R=100m	-4.43	-4.90
		R=700m	-4.52	-5.12
		R=1500m	-4.49	-4.96
	60^G	R=100m	-5.95	-6.58
		R=700m	-6.10	-6.78
		R=1500m	-6.05	-6.63
	without obliquity and curvature		-9.07	-10.43
L=20m opening	40^G	R=100m	-12.11	-8.57
		R=700m	-12.34	-8.69
		R=1500m	-12.27	-8.47
	50^G	R=100m	-17.03	-11.68
		R=700m	-17.41	-11.71
		R=1500m	-17.29	-11.53
	60^G	R=100m	-21.73	-14.63
		R=700m	-22.23	-14.66
		R=1500m	-22.08	-14.51
	without obliquity and curvature		-30.77	-20.87
L=30m opening	40^G	R=100m	-32.18	-16.85
		R=700m	-32.79	-16.75
		R=1500m	-32.61	-16.50
	50^G	R=100m	-43.34	-22.20
		R=700m	-44.20	-21.94
		R=1500m	-43.94	-21.76
	60^G	R=100m	-53.85	-27.12
		R=700m	-54.95	-26.94
		R=1500m	-54.62	-26.78
	without obliquity and curvature		-74.02	-37.40

Table 2. Bending moments from permanent loads on each isolated longitudinal beam from the deck (kNm)

L	Obliquity	Radius	Bending moments from permanent loads (kNm)					
			Beam 1	Beam 2	Beam 3	Beam 4	Beam 5	Beam 6
L=10m opening	40^G	R=100m	107.5	116.2	110.5	111.7	119.9	113.1
		R=700m	111.7	120.4	114.2	115.1	123.2	116
		R=1500m	110.4	119.1	113.1	114.1	122.2	115.1
		Without curve	102.6	111.1	106.1	107.7	116.1	114.3
	50^G	R=100m	188.3	182.3	189.2	184.2	185.2	193.7
		R=700m	195.5	189.1	195.7	190	190.6	199.1
		R=1500m	193.3	187	193.7	188.2	188.9	197.5
		Without curve	179.7	174.4	181.5	177.3	178.8	187.4
	60^G	R=100m	241	247	244.9	245.4	249.3	244.3
		R=700m	250.2	256.1	253.4	253.4	256.9	251.4
		R=1500m	247.4	253.3	250.8	251	254.6	249.2
		Without curve	230.2	236.3	234.9	236.1	240.5	236
	Without obliquity and curve		324.7	354.3	352.4	352.4	354.3	324.7
L=20m opening	40^G	R=100m	900.8	961.7	953.7	954.3	963.9	905.1
		R=700m	924.7	987	978.2	978.1	987.3	926.8
		R=1500m	917.4	979.3	970.7	970.9	980.2	920.2
		Without curve	872.6	932.1	924.8	926.2	936.5	879.7
	50^G	R=100m	1164	1241	1221	1222	1244	1175
		R=700m	1195	1273	1252	1252	1275	1203
		R=1500m	1185	1263	1243	1243	1265	1194
		Without curve	1128	1203	1184	1186	1208	1141
	60^G	R=100m	1382	1548	1484	1485	1551	1390
		R=700m	1419	1589	1522	1523	1590	1424
		R=1500m	1408	1576	1511	1511	1578	1414
		Without curve	1340	1501	1439	1441	1506	1350
	Without obliquity and curve		1912	2094	2091	2091	2094	1912
L=30m opening	40^G	R=100m	2924	3045	3045	3047	3052	2950
		R=700m	2987	3111	3110	3111	3116	3012
		R=1500m	2968	3091	3090	3091	3096	2993
		Without curve	2849	2968	2968	2971	2977	2878
	50^G	R=100m	3529	4160	3691	3876	4179	3431
		R=700m	3605	4250	3770	3958	4267	3503
		R=1500m	3582	4223	3746	3933	4240	3481
		Without curve	3439	4055	3598	3780	4076	3347
	60^G	R=100m	4182	4540	4547	4537	4554	4206
		R=700m	4273	4638	4644	4633	4650	4294
		R=1500m	4245	4608	4615	4604	4621	4267
		Without curve	4076	4425	4433	4423	4441	4102
	Without obliquity and curve		5457	5924	5921	5921	5924	5457

Table 3. Bending moments from LM71 on each isolated longitudinal beam from the deck (kNm)

L	Obliquity	Radius	Bending moments from LM71 (kNm)					
			Beam 1	Beam 2	Beam 3	Beam 4	Beam 5	Beam 6
L=10m opening	40^G	R=100m	130.2	131.3	120.3	116.5	120.2	110.3
		R=700m	131.8	133.5	119.6	115.1	117	106.4
		R=1500m	129.9	132.7	120	116.5	119.8	109.9
		Without curve	125.3	129.7	121.3	121.6	129.6	127.1
	50^G	R=100m	222	204.6	206.2	193.9	189	193.2
		R=700m	225.1	207.8	206	192.3	185.3	188
		R=1500m	222.1	206.4	206.1	193.9	188.4	192.4
		Without curve	203.9	212.7	207.3	207.1	210.1	200.3
	60^G	R=100m	280.3	276.6	267	260.9	258.2	248.3
		R=700m	283.9	280.4	267.5	259.3	254.2	242.9
		R=1500m	280.5	278.9	267.5	260.9	257.5	247.4
		Without curve	272.2	286.9	281	280.5	282.9	267.2
	Without obliquity and curve		383.2	412	399.9	397.9	397.1	362.2
L=20m opening	40^G	R=100m	663.1	694.8	673.3	658.9	653.1	605.3
		R=700m	661.4	692.2	672.6	658.6	652.6	605.1
		R=1500m	656.4	689.6	673.2	661.7	658.4	612.3
		Without curve	654.8	696	692.1	687.8	688.3	643.9
	50^G	R=100m	835.6	878.5	847.4	833.1	835.7	781.2
		R=700m	832.6	871.8	845.9	831.6	833.8	779.6
		R=1500m	827.5	870.1	846.6	834.6	839.6	786.9
		Without curve	829.7	884.8	879.3	875.8	876.4	819.4
	60^G	R=100m	976	1078	1018	1003	1035	919
		R=700m	973.9	1075	1016	1002	1034	918
		R=1500m	968.6	1071	1016	1005	1040	925.1
		Without curve	995.5	1061	1056	1054	1054	985.5
	Without obliquity and curve		1350	1467	1455	1447	1445	1316
L=30m opening	40^G	R=100m	1593	1639	1614	1590	1571	1505
		R=700m	1579	1628	1606	1589	1575	1509
		R=1500m	1571	1620	1606	1594	1584	1520
		Without curve	1569	1704	1700	1696	1696	1561
	50^G	R=100m	1879	2204	1926	1993	2123	1731
		R=700m	1865	2186	1919	1993	2128	1738
		R=1500m	1858	2180	1920	1998	2138	1748
		Without curve	1919	2085	2083	2079	2079	1914
	60^G	R=100m	2200	2378	2348	2316	2302	2114
		R=700m	2185	2356	2340	2313	2304	2117
		R=1500m	2178	2348	2342	2317	2313	2127
		Without curve	2246	2438	2439	2434	2435	2241
	Without obliquity and curve		2866	3098	3086	3074	3067	2819

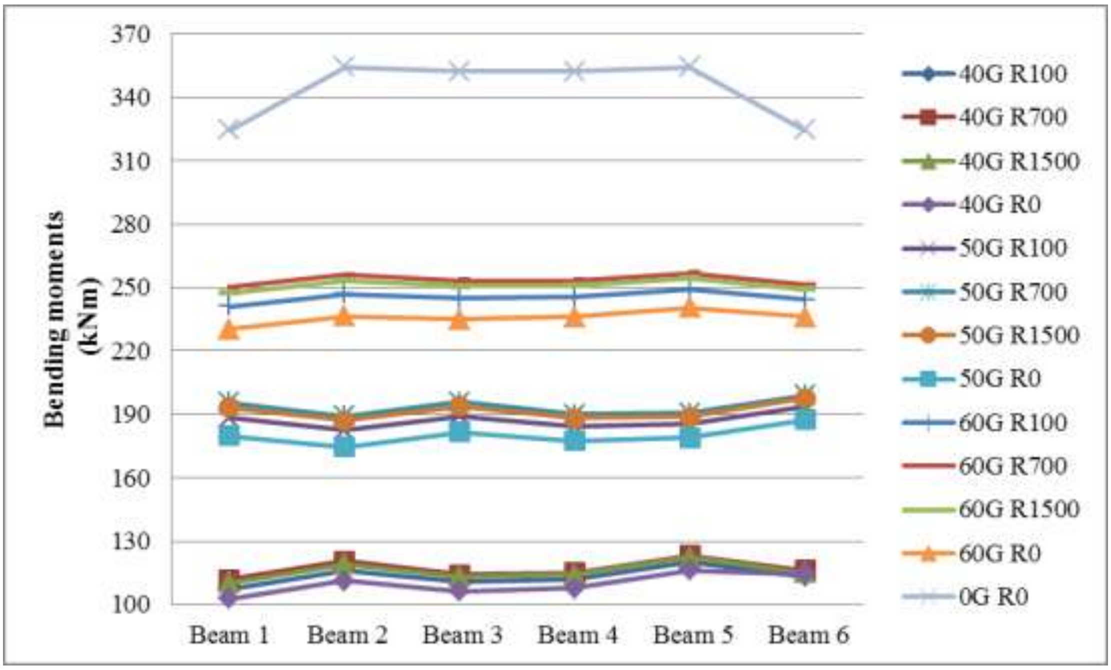

Figure 12. Variation of bending moments from permanent loads in the midspan section for bridge with L=10m span

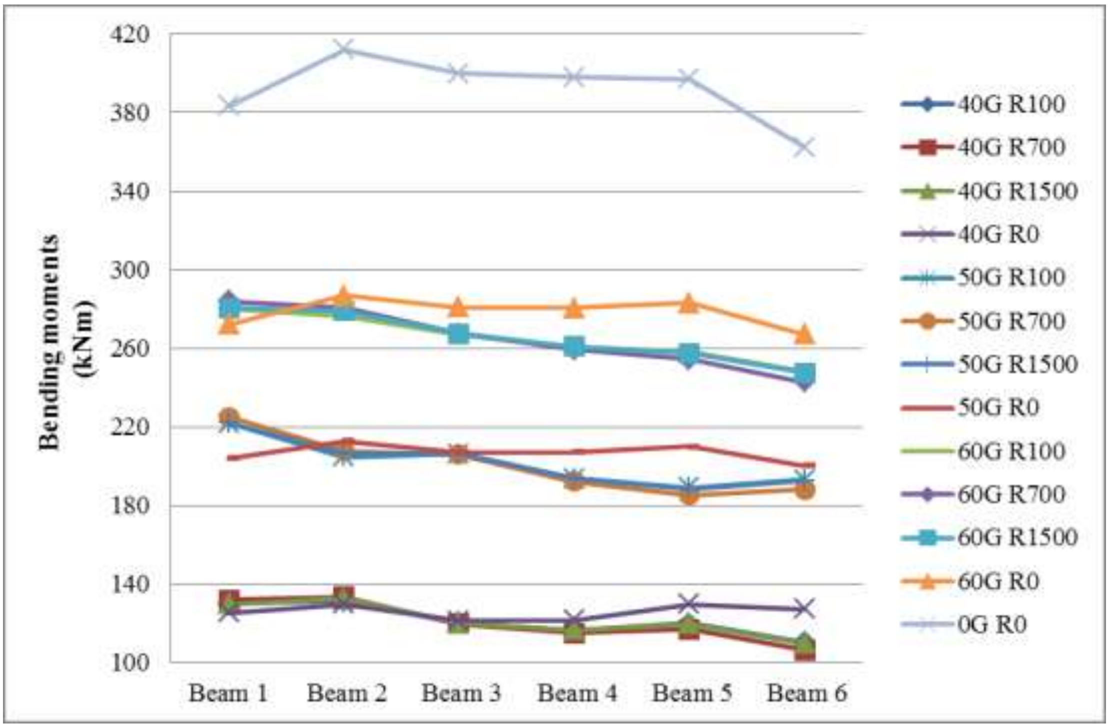

Figure 13. Variation of bending moments from LM71 in the midspan section for bridge with L=10m span

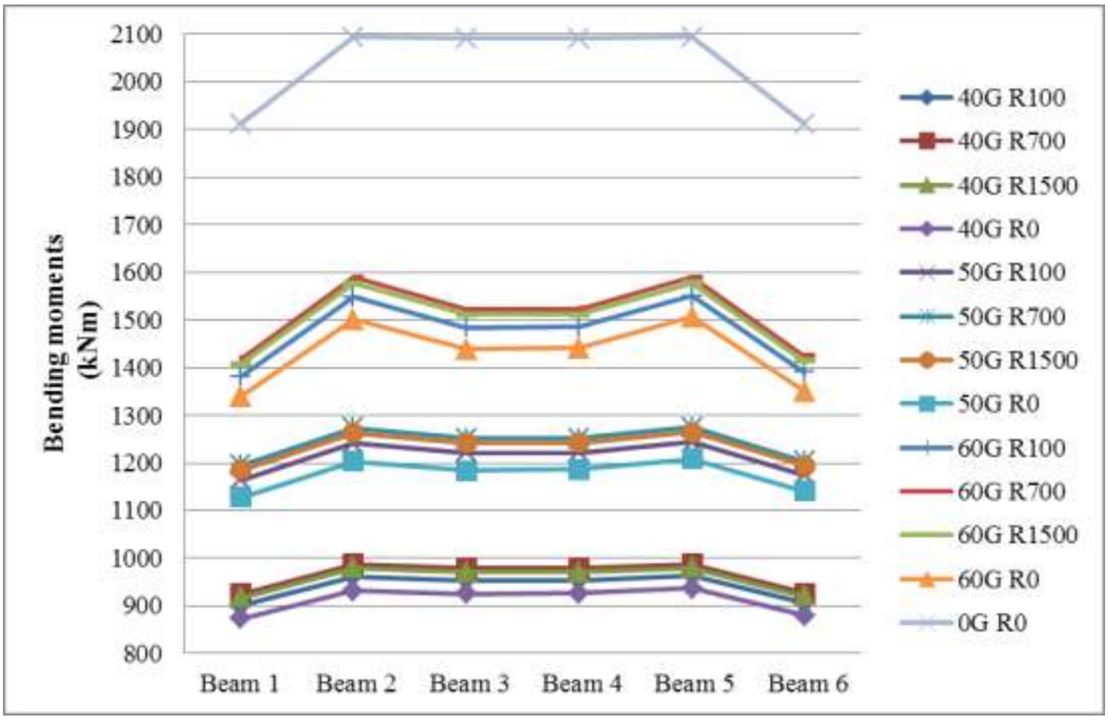

Figure 14. Variation of bending moments from permanent loads in the midspan section for bridge with L=20m span

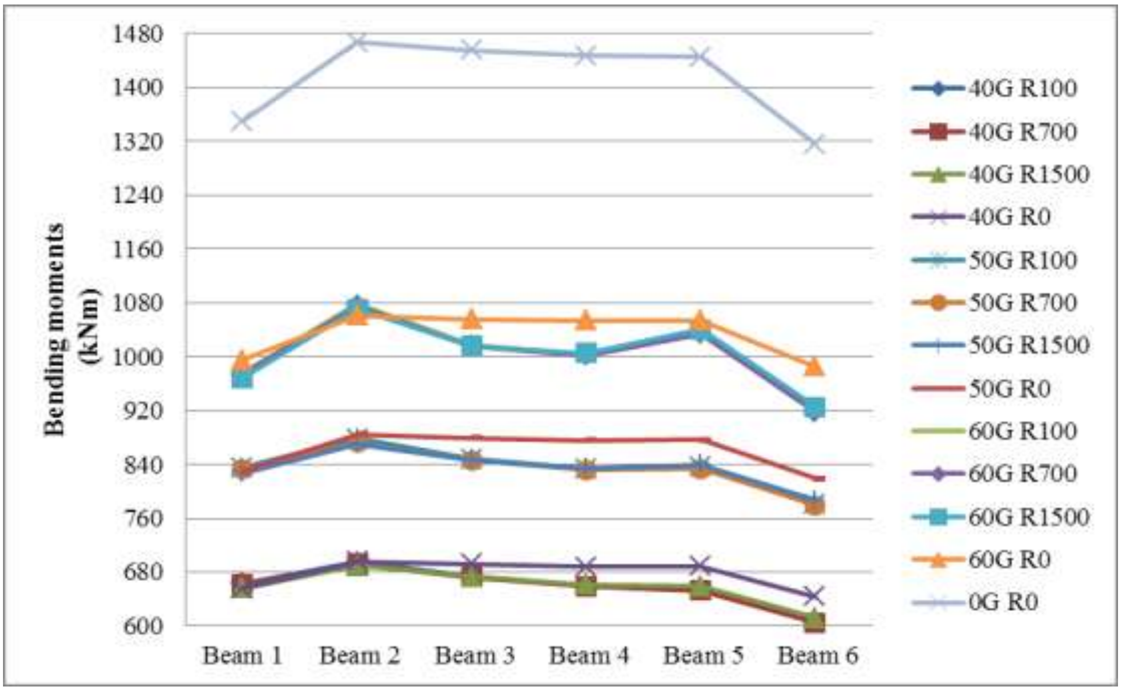

Figure 15. Variation of bending moments from LM71 in the midspan section for bridge with L=20m span

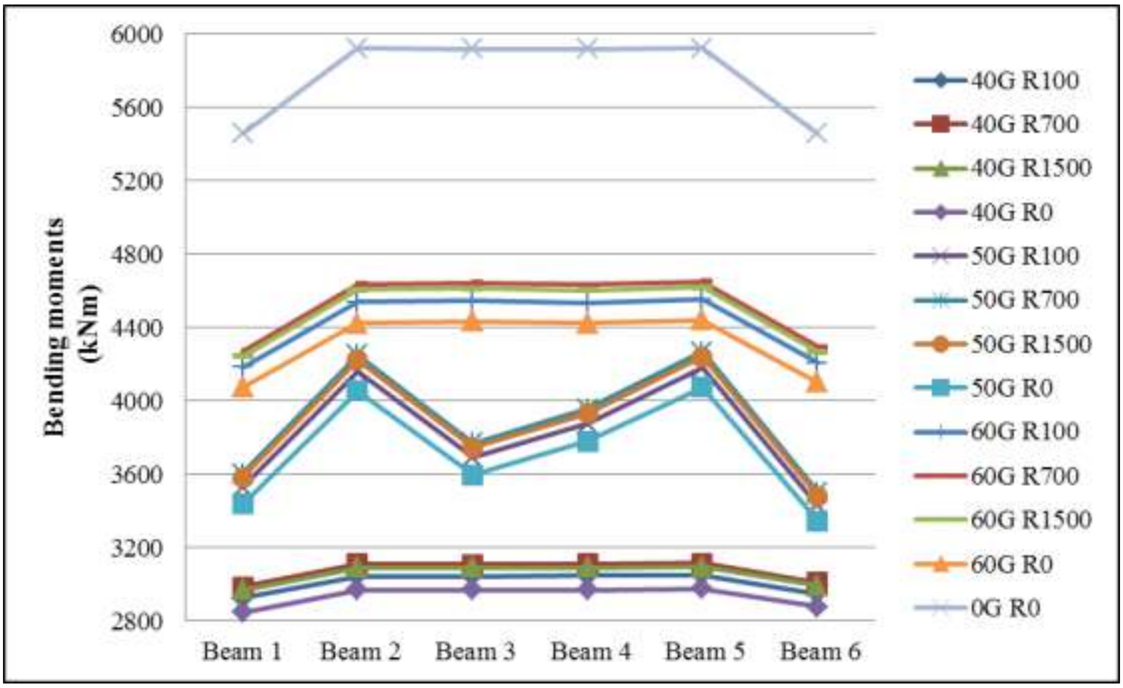

Figure 16. Variation of bending moments from permanent loads in the midspan section for bridge with L=30m span

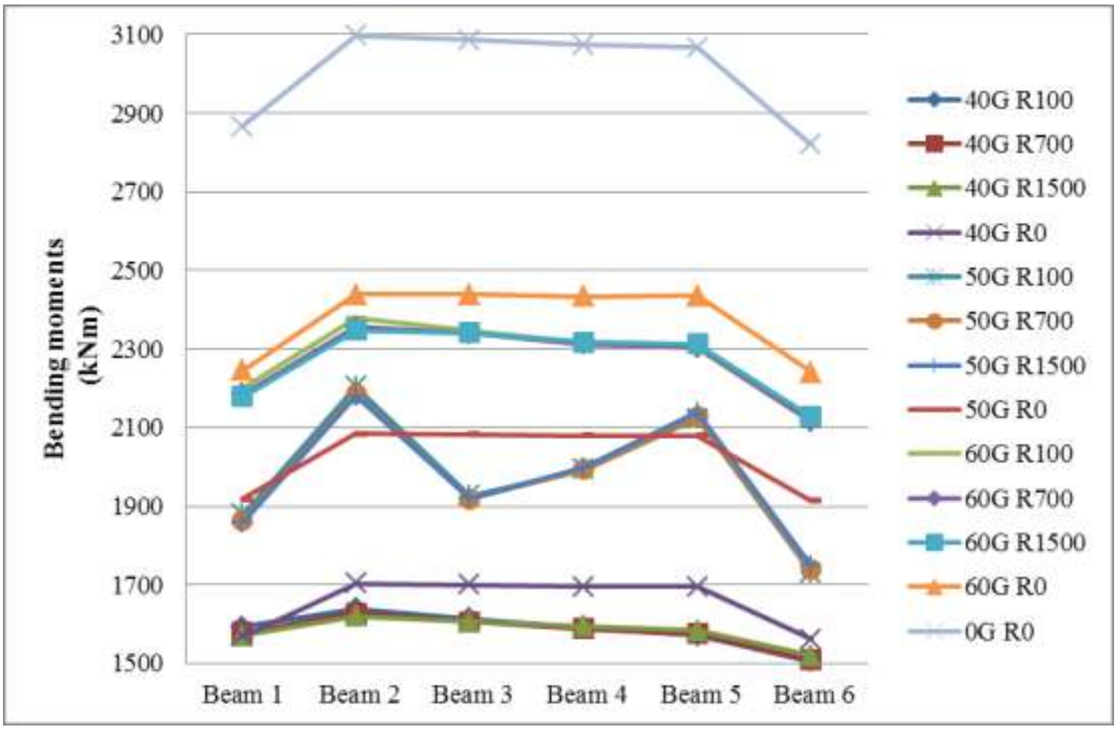

Figure 17. Variation of bending moments from LM71 in the midspan section for bridge with L=30m span

4. CONCLUSIONS

Regarding the maximum deflections of the deck (△Zmax), their values are much lower as compared to those from the situation of bridges without support line obliquity (see Figure 11).

Their values, depending on the support line obliquity, are between 32,8% and 73,5% of those obtained for bridges without support line obliquity. This is normal as with the increase of the support line obliquity the deck becomes more rigid in the longitudinal direction. From the analysis of Table 1, it is observed that the maximum deflection increases with increasing the opening and the support line obliquity.

Regardless of opening and support line obliquity, maximum deflection values occur for a radius of R=700m, for which the values of centrifugal force are maximum.

It can be noted that, regardless of support line obliquity, the maximum bending moment at small openings occurs for the radius R=700m, for which the centrifugal force is maximum. With the increase of the opening, the maximum value of the bending moment occurs for the radius R=100m, because, geometrically, the external forces are moving away from the axis of the deck.

The fact that the track axis is curved on the bridges with support line obliquity does not significantly change the values of the bending moments. An increase in the maximum bending moment of about 5% is recorded in the case of the bridge with 10m opening, 3% in the case of the bridge with 20m opening and 2% in the case of the bridge with 30m opening, as seen/shown in Figure 18.

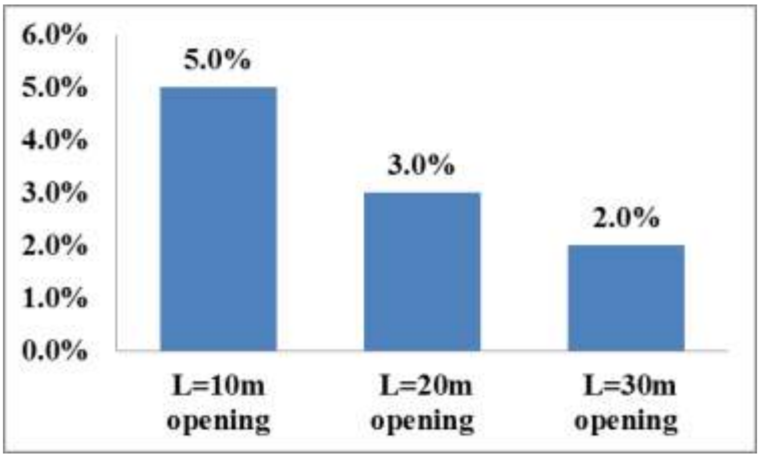

Figure 18. The increase of maximum bending moment due to track axis curvature presence on bridges with support line obliquity

The overall conclusion is that the support line obliquity dictates the behavior of the analyzed structures, the presence of the curve does not significantly influence the results that were compared. In the case of bridges with support line obliquity there is a great deal of stress in the support zones on the short diagonal of the deck. So, great care must be taken in the design of the supports and of the end zones on the short diagonal of the deck.

REFERENCES

[1]. ***, “*UIC Code 773-4 R*”, International Union of Railways, F-75015 Paris, **1997**

[2]. ***, EN 1992-1-1:2004, “*Eurocode 2: Design of concrete structures - Part 1: General rules and rules for buildings*”, **2004**

[3]. ***, EN 1994-2:2005, **“***Eurocode 4: Design of composite steel and concrete structures – Part 2: General rules and rules for bridges***”**, **2005**

[4]. ***, “*Element Reference Manual*”, LUSAS Finit Element Analysis, Version 15.0

[5]. STĂNESCU R.M., “*Study of influence of the track curvature and supports obliquity at railway bridge structures with steel beams embedded in concrete*”, PhD. Thesis, T.U.C.E. Bucharest, Romania, **2016**

[6]. GIORDANO A., RĂCĂNEL I.R., VOIRO G., “*Steel-concrete viaducts in the Orăştie-Sibiu Highway: a Eurocode compliant project*”, The VI-th INTERNATIONAL SCIENTIFIC CONFERENCE Road Research and Administration, pp 1183-1194, www.cfdp.utcb.ro/car, “CAR 2013”, Bucharest**, 4-5 July 2013**

[7]. RĂCĂNEL I.R., MUTU C.S., “*Strengthening of the cable-stayed bridge over Danube at Agigea*”, Seven-th Conference on Bridge Maintenance, Safety, Management and Life Extension I.A.B.M.A.S. 2014, pp. 2322-2329, ISBN CD-ROM 978-1-138-00103-9, Taylor&Francis Group, Shanghai 7-11 of July, Shanghai, China, **2014**

[8]. RĂCĂNEL I.R. , STOICESCU G., “*Analysis of the stress state for rails with holes near joints*”, 4th European Conference of CIVIL ENGINEERING (ECCIE '13), pp 129-135, http://www.wseas.us/elibrary/conferences/2013/Antalya/MINEC, Antalya, Turkey, **October 8-10, 2013**